Macromolecules
ARTICLE

Macromolecules **2010**, *43*, 409–417 **409**
DOI: 10.1021/ma901666v

Relaxation Kinetics of Nanostructures on Polymer Surface: Effect of Stress, Chain Mobility, and Spatial Confinement

Hua-Gen Peng, Yen Peng Kong, and Albert F. Yee*

Department of Chemical Engineering and Materials Science, University of California, Irvine, California 92697

Received July 28, 2009; Revised Manuscript Received October 12, 2009

ABSTRACT: Relaxation and chain dynamics of polymer nanostructures after release of spatial confinement were studied using line gratings as small as 33 nm on polystyrene surface fabricated by nanoimprint lithography. The temperature for "slumping"—rapid line height relaxation—decreased as the line width diminished for all molecular masses (MWs), but a simple explanation based on enhanced surface mobility fails to explain the results. When MW was low and the structure was large, the line height monitored with an AFM reduced as surface tension overcame the polymer viscosity. Interesting and complex behaviors were observed when the radius of gyration (R_g) of the polymer molecules was not small compared with the dimension of the nanostructure. Careful examination of the surface viscosity shows that confinement of polymer chains into space comparable to or even smaller than its R_g appears to enhance relaxation, which is the major factor for the surprisingly low temperature at which nanostructures of high MW slumps.

Introduction

The surface of polymers has been an arena for a host of unique and interesting observations. For example, it is widely believed that the surface causes polymer thin films to dewet and rupture at temperatures significantly below the bulk glass transition temperature ($T_{g\infty}$)[1] and to reduce the T_g of supported[2,3] and free-standing thin films.[4] Many hypotheses have been advanced and simulations performed to argue that the surface is more mobile than the bulk.[5−8] Experimental evidence of enhanced mobility, at least on the segmental level, has been widely reported.[9−12] Among all the evidence of enhanced surface mobility, the mobility of molecular chains is still a subject of some controversy. As well summarized in these reviews,[13,14] some experimental results suggest that mobility of entire molecules is essentially unchanged or even reduced.

The nature of the polymer surface can be expected to affect the stability of polymer structures in nanoscales, where the surface to volume ratio is relatively high. Polymers are now being patterned into nanometer-sized structures in a wide range of applications, e.g., electronics, sensors, photonics, and photovoltaics. Robust mechanical stability or the ability to predict the relaxation behavior of these nanostructures is critical for their performance, especially for applications intended for long-term use. With the assumption of a mobile surface, the stability of polymeric nanostructures is expected to be reduced with decreasing feature size, as the surface to volume ratio increases. However, very little research into the stability of polymeric nanostructures has been done. There are observations that surface nanostructures can relax rapidly even at temperatures below the bulk $T_{g\infty}$.[15−17] In such cases, one would expect the relaxation rate should be strongly dependent on the size of the polymer structure. However, nanometer-sized holes in the polymer surface were found to relax at the same speed as the protruding rims of much larger radius of curvature.[15] On the other hand, poly(methyl methacrylate) (PMMA) lines 50 nm in width proved to be quite stable as they sustained annealing at 25−30 deg above the bulk $T_{g\infty}$ without perceivable shrinkage, contradictory to all the observations above.[18] These discrepancies in the mechanical stability of polymeric nanostructures warrant further systematic research in order to arrive at a better and consistent understanding. Such understanding concerns not only polymeric nanostructures but also patterning techniques such nanoimprinting, which proves successful in creating structures as small as 10 nm with glassy polymers (e.g., PMMA).[19]

One important question regarding nanostructure stability is whether the viscosity of thin films or surfaces is different from that of the bulk. If the surface is indeed mobile, its viscosity should be lower than that of the bulk; however, there are also controversies in this regard. Bodiguel[20] and Green[21] argued for reduced viscosity in polymer surface and ultrathin films from observing thin film dewetting behavior, while Johannsmann[22] and Kim[23] concluded from surface wave measurement that the surface viscosity was no lower than the bulk value. Dutcher et al.[24] found that the viscosity of free-standing films decreased with decreasing film thickness and interpreted the reduced viscosity as the result of shear thinning. Another important and interesting question is, if the size of the nanostructure is close to or smaller than the size of the polymer molecular coil, how would this influence the structure stability? In this paper this factor will be referred to as the size effect, which is akin to a confinement effect. The size effect would be expected to give rise to entropic changes. We would not expect it to manifest itself at temperatures far below the bulk $T_{g\infty}$ as the relaxation rate is slow. As the temperature increases, the rate of various relaxation modes in the polymer condensed phase should increase, causing the viscosity and mechanical modulus to decrease. But, as the structure size (or feature size) decreases, the surface to volume ratio increases at the same time as the size effect becomes stronger. Therefore, careful experimental design and analysis are needed if the convoluted effects are to be resolved.

In this work, nanoimprinting is used to create surfaces with well-defined feature shapes and sizes, while AFM is used to study the stability of these features fabricated from polystyrene of different molecular masses. The hope is that the work presented here can also shed further light on the nature of surface mobility and help resolve the controversies.

*Corresponding author. E-mail: afyee@uci.edu.

Published on Web 11/06/2009

Experiment

Materials. Polystyrene (polydispersity index 1.03−1.05) was purchased from Polymer Source (MW = 6.4, 15.5, 41.5, and 220.9 kg/mol) and Scientific Polymer Products (MW = 1571 kg/mol). For simplicity, polystyrene of these five MWs will be designated as PS6k, PS15k, PS41k, PS220k, and PS1571k, respectively. Toluene (Certified ACS), as the solvent of polystyrene for spin-coating, was purchased from Fisher Chemical.

Film Preparation. The majority of the samples were made by reversal nanoimprint lithography (r-NIL). The details of the r-NIL technique have been given in previous publications.[25] Briefly, a Si mold was plasma cleaned and coated with a layer of 1*H*,1*H*,2*H*,2*H*-perfluorodecyltrichlorosilane (FDTS) to provide it with a low-energy surface, while the Si substrate used to support the polymer film was cleaned with piranha solution, leaving an intrinsic silica layer. PS dissolved in toluene was spin-coated onto the Si mold (see Table 1 and Figure 1), followed by a soft bake at 115 °C for 5 min to remove residual solvent, and then a flat Si substrate was used to sandwich the polymer film between substrate and mold. Then the assembly was inserted into a nanoimprinter (HEX 03, Jenoptik). The sandwiched polymer film was heated to 150 °C under vacuum in 5 min, and then a pressure of 5 MPa was applied. A typical imprinting condition was 150 °C for 10 min. After imprinting and while still under pressure, the film was cooled to below $T_{g\infty}$ in 2 min and cooled further to 60 °C before the imprinter pressure was reduced to zero. Then the film was further cooled to room temperature before the mold was opened. The low surface energy of the FDTS-coated Si mold caused the PS film to be transferred and attached onto the flat Si substrate. Adhesion between the film and the Si substrate was sufficient to prevent any dewetting from occurring in these experiments.

Table 1. Detailed Information of the Polystyrene Line Grating Patterns

feature size	period (λ)	height
~33 nm	200 nm	44 nm
~300 nm	700 nm	262 nm
600 nm	1.2 μm	500 nm
8 μm	16 μm	1 μm

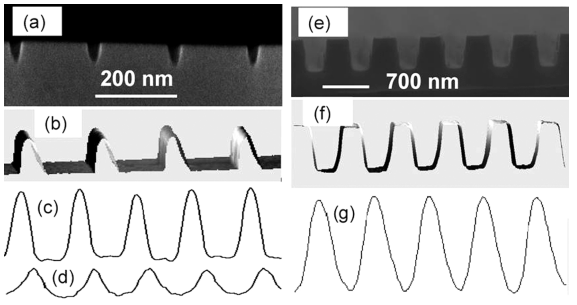

Figure 1. Cross-section SEM micrographs of the Si molds (a, e: Si is the bottom half of the graphs) and AFM scans (three-dimensional view at the cross section) of the polystyrene film (b, f) for the 30 and 300 nm features, respectively. The width of the lines in AFM scans appears to be slightly broadened by the shape of the AFM tip. Line height in AFM scan (c) is 20 nm at an earlier slumping stage of a 30 nm grating; height in scan (d) is only 6 nm for the same film at a later slumping stage. Line height in scan (g) of a 300 nm grating is 90 nm, at a later stage of slumping.

To observe the effect of thermal history on nanostructure stability, a modified process, conveniently called "peel-off", was also employed. In the peel-off process, after the polymer solution was spin-coated onto the mold, the resulting film was simply annealed on a hot plate or in a vacuum oven before it was peeled off the mold and laid on a flat silicon wafer, with the side containing the nanostructure facing up. (The opposite side was flat). This peel-off process was used only on PS1571K. The specimens and their preparation conditions are summarized in Table 2.

Table 1 lists the specification of the four molds used in this work. These molds have feature sizes ranging from 33 nm to 8 μm. The mold with trench width 8 μm was purchased from NTT Advanced Technology, catalog #NIM-1000UL. The molds with trench widths 600 and 33 nm were made from e-beam lithography, and the mold with trench width 300 nm was made by interference lithography. The top of the 33 nm lines was rounded owing to the small size and the reactive-ion-etch (RIE) step in Si mold preparation; the line tops of the other molds were flat, with rounded edges of much smaller radii than the feature sizes. Figure 1a,e shows the SEM cross-section micrographs of the silicon molds with 33 and 300 nm wide trenches, while Figure 1b,f shows a small patch of the AFM scan of the polymer films made with these two molds. One important aspect of all the specimens is that the overall film thickness was on the order of micrometers, thus significantly larger than the height of the line features. Therefore, the behavior of the nanofeatures can be considered largely free from substrate effects.

AFM Measurement. A noncontact atomic force microscope with an enclosed sample chamber (NTEGRA Therma, NT-MDT) was used to observe the decay of the pattern while the sample pattern was exposed to elevated temperatures stepwise through glass transition. This AFM system has very low thermal drift characteristics and allows reliable quantitative topographical measurements at stable temperatures. The line height was the major physical quantity measured for a relatively fixed scan area. The first type of measurement conducted was to find the temperature at which the pattern started to relax rapidly, or "slump". This temperature, which we shall designate T_s, was expected to be dependent on the rate of heating. The measurement temperature began at room temperature, which was then raised in 10°−20° steps. When noticeable height decrease began to be observed—typically several nanometers—smaller

Table 2. Film Identification (ID) and Preparation Condition

PS MW (kg/mol)	size	film ID	short description
1571	33 nm	1571k-33nm-rNIL-150C	reversal nanoimprinting at 150 °C for 10 min
		1571k-33nm-rNIL-195C	reversal nanoimprinting at 195 °C for 10 min
		1571k-33nm-Peel-115C	peel-off after annealing at 115 °C for 10 min
		1571k-33nm-Peel-180C	peel-off after annealing at 180 °C for 24 h in vacuum
	300 nm	1571k-300nm-rNIL-150C	reversal nanoimprinting at 150 °C for 10 min
		1571k-300nm-Peel-180C	peel-off after annealing at 180 °C for 24 h in vacuum
		1571k-300nm-Peel-190C	peel-off after annealing at 190 °C for 48 h in vacuum
		1571k-300nm-Peel-155C	peel off after baking at 155 °C for 10 min on a hot plate
	600 nm	1571k-600nm-rNIL-150C	reversal nanoimprinting at 150 °C for 10 min
	8 μm	1571k-8μm-rNIL-180C	peel-off after annealing at 180 °C for 24 h in vacuum
220.9[a]	33 nm	220k-33nm-rNIL-150C	reversal nanoimprinting at 150 °C for 10 min
	300 nm	220k-300nm-rNIL-150C	reversal nanoimprinting at 150 °C for 10 min
	600 nm	220k-600nm-rNIL-150C	reversal nanoimprinting at 150 °C for 10 min

[a] For PS41k, PS15k, and PS6k, the same set of films were prepared using the same reversal nanoimprinting condition. For example, the set for PS41k is 41k-33nm-rNIL-150C, 41k-300nm-rNIL-150C, and 41k-600nm-rNIL-150C.

temperature steps of 1°−3° were used. The temperature was raised to and stabilized at the target value in 2 min and held for 20 min for thermal equilibrium to be established. By measuring the line height stepwise, the slumping onset temperature could be found. This type of measurement program is denoted here as "H-Temp" measurement where H is the height. In the second set of measurement program, designated as "H-Time", a fixed temperature at or above T_s was chosen, and the line height reduction with time was monitored. As will be shown in Results and Discussion sections, the slumping dynamics and viscosity of the film (or the surface) can be deduced from H-Time measurements.

Results

The slumping onset temperature (T_s) is used here as the critical parameter to indicate the thermal stability of the nanostructure. T_s is defined here (Figure 2) as the intercept between two lines, one on the $T < T_s$ side where the normalized line height is almost constant and the other on the $T > T_s$ side where the height quickly diminishes with the increase in temperature. As can be seen in Figure 2, T_s decreased with decreasing line width for PS41k. The 600 nm lines started to slump at about 107 °C, the 300 nm lines at 104 °C, while the 33 nm lines slumped at 94 °C, 3° lower than the glass transition temperature of the bulk polymer, $T_{g\infty}$ (97 °C). This trend is observed for all the MWs investigated (Table 3). The results in Table 3, which are based on the average of triplicate measurements, show that the stability of nanostructures on polymer surface decreases with the feature size, as expected. On the other hand, the MW dependence of T_s seems rather complicated. Taking the 600 nm films for example, T_s of PS1571k agrees well with $T_{g\infty}$, while T_s of PS6k occurs 10 deg above the bulk $T_{g\infty}$.

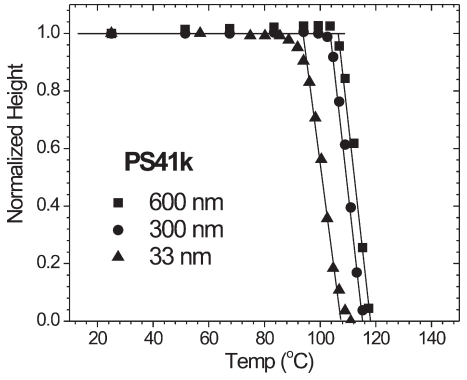

Figure 2. Normalized height of PS41k line gratings vs temperature. All the films were prepared by rNIL at 150 °C.

Table 3. Slumping Onset Temperature (T_s) of Polystyrene of Different MWs and Feature Sizes in Line Grating Patterns[a]

			T_s (°C)		
PS MW (kg/mol)	R_g[b] (nm)	DSC[c] (°C)	600 nm	300 nm	33 nm
1571	72	104.9	105	105	99
220.9	27	104.4	105.5	100−102	97−98
41.5	11.7	96.8	106.5	103.5	94
15.5	7.2	92.7	102.5	101.5	94.5
6.4	4.6	83.4	94.5	93.5	75.5−76

[a] All the specimens in this table were made with reversal nanoimprinting, molded at 150 °C, and held for 10 min. T_s results are averaged from triplicate measurements and have a range of ±0.5 °C. [b] Radius of gyration is calculated using the parameter under the theta condition: *Polymer Handbook*, 4th ed.; Brandrup, J., Immergut, E. H., Grulke, E. A., Akihiro, A., Bloch, D. R., Eds.; John Wiley & Sons: New York, 1999. [c] Differential scanning calorimetry was performed on Q100, TA Instrument at a heating rate of 10 °C/min.

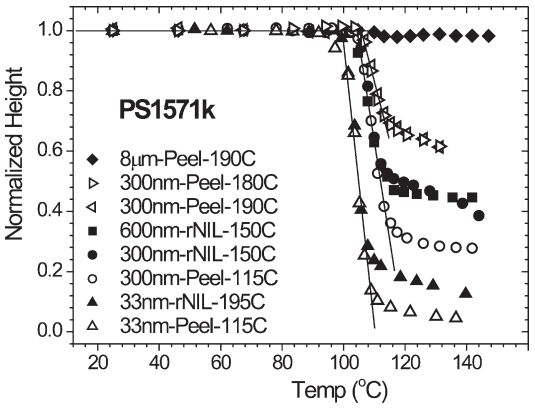

Figure 3. Normalized height of PS1571k line gratings vs temperature from H-Temp measurements.

To unravel the T_s dependence on feature size, the effect of process history of the line gratings on T_s was also examined. Residual stresses could have arisen during two stages in the process, namely, spin-coating and transfer under pressure of the film from the mold to the Si wafer. Residual stress would reduce T_s if film annealing is not sufficient. H-Temp curves of PS1571k gratings of various sizes and annealing conditions are shown in Figure 3. Some films were prepared with r-NIL as described above, while others by the "peel-off" process. There is no statistically significant difference between these two sets of films in terms of line height despite the absence of transfer pressure and different annealing temperatures in the latter. This means that the transfer step in r-NIL did not introduce additional residual stress. A fortunate consequence is that films prepared by either r-NIL or "peel-off" can be directly compared simply based on the temperature used. The terminal relaxation times of PS6k, PS15k, and PS41k at 150 °C should be orders of magnitude shorter than 10 min, which was the dwell time before transfer. Therefore, the set of films with these low MWs should be free of residual stress due to molecular orientation. However, for PS of higher MWs, especially PS1571k, the dwell at 150 °C for 10 min may not have been sufficient for removing in its entirety what residual chain orientation that may have arisen from the spin-coating process. Indeed, the curves in Figure 3 demonstrate that annealing does result in different slumping behaviors for the higher MW PS1571k nanostructures.

Comparing Figure 3 and Figure 2, one immediately notices that PS1571k H-Temp curves (except the 8 μm lines) have an interesting plateau following a rapid decrease in line height within a 10° temperature window after slumping starts. The annealing history clearly has a stronger influence on the plateau height than on T_s. For example, 1571k-33nm-Peel-115C and 1571k-33nm-rNIL-195C have virtually the same T_s, even though the latter is expected to have more residual stress and the former none at all. Thus, T_s cannot be used to distinguish between the two line structures even though they have such a drastic difference in thermal history. As will be shown in the Discussion, there is a more dominant factor dictating T_s for 1571k-33nm than residual stress. It should be noted that annealing at 195 °C for 10 min does raise the plateau from ~5% in normalized height to more than 10% or from 2~3 nm to 6 nm in terms of absolute line height. Such a large change in the plateau position is also observed in the 1571k-300nm films. The plateau of 1571k-300nm-Peel-115C is at less than 30% in normalized height or ~80 nm, while that of 1571k-300nm-Peel-190C is at more than 60% or 160 nm. With such a large difference in the plateau value, the T_s of these two structures nevertheless differ by only 2°. This comparison suggests again that another more dominant factor may be at play in controlling T_s.

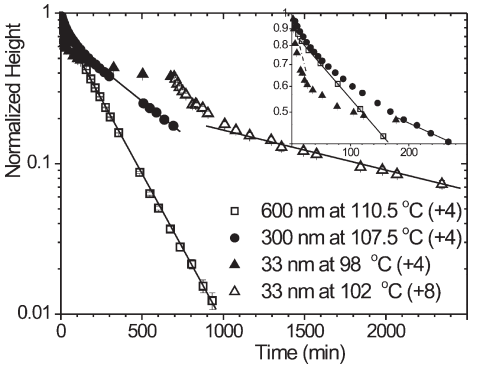

Figure 4. Normalized height of PS41k line gratings vs time from H-Time measurements. The line widths and measurement temperatures are shown in the legend. The number in parentheses shows the difference between the T_s and H-Time measurement temperature. All the films were prepared by rNIL at 150 °C. The inset shows the results of the first 300 min.

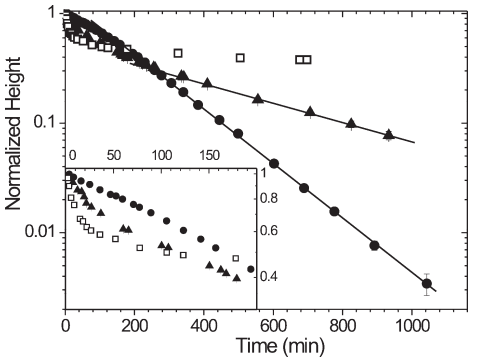

Figure 5. Normalized height of PS15k 300 nm (●, at 103 °C) and 33 nm (▲, at 98 °C) line gratings vs time from H-Time measurements. The □ symbol is the H-Time result of PS41k-33 nm (at 98 °C). All the films were prepared by rNIL at 150 °C. The inset shows the results of the first 200 min.

One property that should play a dominant role in T_s is viscosity. As temperature rises through glass transition, the viscosity of PS decreases by orders of magnitude. One understanding of T_s could simply be that at this temperature the slumping driving forces (e.g., surface tension) start to overcome the viscosity. Therefore, measurements to estimate the viscosity are crucial for understanding the complex T_s dependence on line width and MW in Table 3.

For simple sinusoidal surface waves of a viscous liquid, the amplitude of the surface wave decays exponentially with time, and the time constant τ is given by[22,26]

$$\tau = \lambda\eta/(\pi\gamma) \quad (1)$$

where λ is the wavelength, η the viscosity of the film (or surface), and γ the surface tension. The plot of relative wave amplitude in logarithmic scale vs linear time is a straight line for a simple exponential decay, and the reciprocal of the absolute slope is the time constant τ. Figure 4 shows such a plot for the H-Time measurement of the PS41k films. It should be noted that the initial cross section of the surface structures produced by the imprinting method is closer to being trapezoidal than sinusoidal. Nonetheless, the cross-sectional profile after significant slumping became sinusoidal for the 300 and 600 nm lines, which is consistent with surface tension being part of the driving force (see Figure 1g). The fitted straight lines show that the surface wave indeed decays exponentially with time except for the faster than exponential slumping in the beginning. Such behavior has also been reported in other studies on polymer nanostructures.[22,26] As

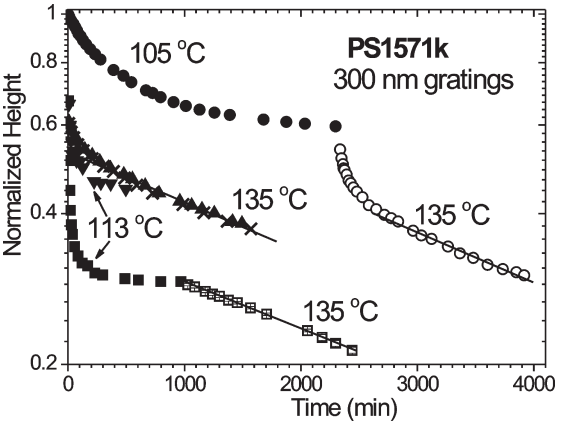

Figure 6. Normalized height of PS1571k-300 nm line gratings (▼ rNIL-150C; □, ■ Peel-115C; ▲ Peel-190C; ●, ○ Peel-155C; × Peel-180C) vs time from H-Time measurements. The measurment temperatures are shown in the legend. The results of Peel-180C and Peel-190C were collected after H-Temp measurement concluded at 130 °C.

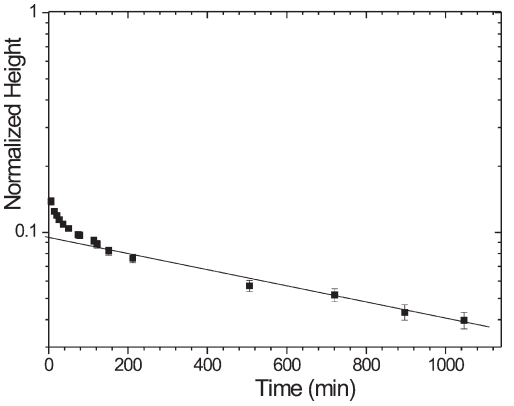

Figure 7. Normalized height of PS1571k-33nm-Peel-180C vs time from the H-Time measurement at 135 °C.

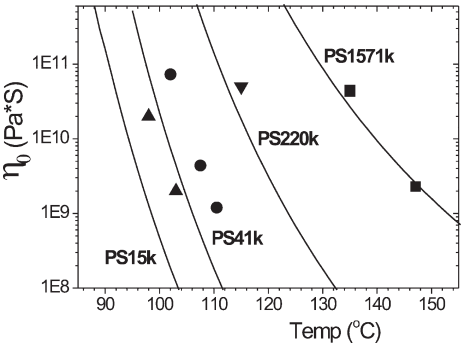

Figure 8. Viscosity calculated (symbols, PS15k ▲, PS41k ●, PS220k ▼, and PS1571k ■) from the linear regime of H-Time measurements in Figures 3−7 vs the bulk zero shear viscosity (lines). There are five measurements at 135 °C for PS1571k on 33 and 300 nm gratings.

will be shown later, the time constant for the exponential decay regime in Figure 4 for PS of all other molecular masses studied is much longer than the terminal relaxation time for PS at the given temperature. It appears reasonable that in such a case PS can be treated as a viscous liquid and the H-Time measurement can be used to calculate the viscosity. From the time constant of the surface wave amplitude decay, the viscosity can be obtained by rearranging eq 1:

$$\eta = \pi\gamma\tau/\lambda \quad (2)$$

The H-Time measurement for PS15k is shown in Figure 5 and for PS1571k in Figures 6 and 7.

The deduced viscosity from the slope of the fitted straight lines in Figures 4−7 is plotted in Figure 8, along with the bulk viscosity calculated from the Vogel−Fulcher−Tamman (VFT) model using parameters obtained from ref 27. As can be seen, the agreement between the estimate here and the bulk data for PS220k and PS1571k is very good. However, the calculated viscosities of PS15k and PS41k are 1 order of magnitude higher than those of the bulk. A possible explanation of the cause for the difference is offered in the Discussion section.

Discussion

From the observation of lowered T_s with decreasing line width in Table 3, it is tempting to draw the conclusion that there exists a mobile surface layer, which decreases T_s as the feature size decreases because the surface to volume ratio increases. However, the full set of results from the entire range of molecular masses presented here suggest that there may be other, more dominant causes for the observation. The first is surface tension; the second is the spatial confinement of the polymer coils.

To arrive at a consistent interpretation of the full set of results presented here, it is important to understand the physical basis for T_s. Clearly, it is associated with the glass transition process. Indeed, the imprinted patterns began to slump in the vicinity of bulk $T_{g\infty}$ for the films listed in Table 3. This is understandable as the modulus and viscosity of polystyrene decreases orders of magnitude across the glass transition regime, and thus the nanostructures would no longer be able to maintain their shapes if a force is applied. In work by other researchers the change of the surface structure with time well below the bulk T_g was discussed in terms of some molecular mode of relaxation.[15,17] However, the slumping process observed here might be simply viewed as the consequence of slumping driving forces overcoming the viscosity of the polymer, recognizing that viscosity is a manifestation of segmental relaxation. In other words, T_s is not directly related to $T_{g\infty}$ (or surface T_g); instead, it is related to the stress in the line grating structure and the viscosity at such a level of stress. This argument seems reasonable in cases where the viscosity at T_s is relatively low, e.g., on the order of 10^9 Pa·s or less for bulk polystyrene. On the other hand, this argument might seem improbable for films of high MWs, whose bulk viscosity is extremely high at T_s, on the order of 10^{13} Pa·s or more. In those cases, the possibility of other relaxation mechanisms must be considered.

For viscous flow to be possible at T_s there must be driving forces. One obvious force is the surface tension, which acts to minimize the surface area. Other driving forces may include the entropic force from molecular orientation and/or confinement and residual stress owing to the film preparation process. Surface tension of polymers is weakly dependent on molecular mass and temperature. For the range of MWs and T_s studied, the surface tension of PS ranges from 32 to 34 mN/m based on empirical equations.[28] For the sake of simplicity, 33 mN/m will be used in the calculations here.

The bulk viscosity of PS6k at T_s = 94.5 °C for 600 nm lines is 5×10^7 Pa·s.[27] This viscosity is quite low, lower than that of pitch at room temperature, as expected for a low MW PS at a temperature 10 deg above $T_{g\infty}$. If a sinusoidal surface wave of a viscous liquid with viscosity 5×10^7 Pa·s is considered, following Johannsmann[22] and Soles,[26] its amplitude would exponentially decay with a time constant of about 500 s based on eq 1; i.e., the amplitude of the wave would decrease to $1/e$ of the initial amplitude in about 8 min. However, the strain over ~22 min at T_s (see Experiment; 20 min is the waiting time for thermal equilibration before the start of AFM scan, plus half of the scan time) is no more than ~5%, which is equivalent to a slumping time constant of about 3×10^4 s. This comparison suggests that the apparent viscosity of PS6k surface is about 2 orders of magnitude larger than the bulk viscosity at the same temperature. This statement may appear surprising, but if it were not true and the surface viscosity was the same as the bulk or even smaller, the analysis above would suggest that the lines would slump at a much lower temperature than the observed T_s. Such surface induced viscosity increase for low MW glassy polymers has been observed before.[22] The enhanced surface viscosity of PS15k and PS41k (Figure 8) also corroborates the observation on PS6k. Our experimental evidence and analysis contradicts the mobile surface layer interpretation, which would be consistent with *lower*, rather than higher, viscosity than the bulk. Therefore, the interpretation of lowered T_s with decreasing line width cannot be based on the mobile surface hypothesis.

One may argue that polystyrene cannot simply be treated as a viscous liquid, where relaxation (or segmental or molecular rearrangement) is not being considered. In fact, segmental relaxation time is at least 2 orders of magnitude faster than the time constant for the surface wave decay in this case. For comparison, the terminal relaxation time, which is given by the product of the zero shear viscosity and equilibrium recoverable compliance, may be calculated:

$$\tau = \eta_0 J_e \tag{3}$$

Using data in the literature,[27,29] the terminal relaxation time for PS6k at 94.5 °C, determined from eq 3, is calculated to be about 5 s. This means that during the surface wave decay of PS6k the rearrangement of the chain segments and molecules occurs at a rate 2 orders of magnitude faster; therefore, this low molecular mass PS can be simply considered a Newtonian liquid, just like small molecules. This may not be true for the large molecular mass PS, as will be examined later.

Now it can be said with confidence that the T_s of the 600 nm lines for PS6k is dictated by the stress from surface tension and its viscosity. In fact, the surface viscosity turns out to be 2 orders of magnitude higher than the bulk. When the line width is reduced to 300 nm, T_s decreases by about 1 °C compared to PS6k-600 nm, corresponding to a viscosity increase of about 40%. Meanwhile, the stress from surface tension is about twice as large as in the narrow lines. Therefore, the decrease in T_s by reducing the line width from 600 to 300 nm can be interpreted simply as the increase in stress from surface tension, not because of the increase in surface to volume ratio. If a similar estimate on the decay rate is done on the 300 nm film, the conclusion would be that the surface viscosity is also about 2 orders of magnitude larger than what is expected from the bulk. Notwithstanding the foregoing, the possibility that there is a very thin surface layer on the order of a couple of nanometers on the polymer surface remains. The nanometer-thick mobile surface layer may well be tethered to the more rigid layer beneath it. Yet, this mobile layer apparently does not contribute to the decrease of T_s in the 300 nm lines. However, such a nanometer-thick surface layer might play a more significant role in the 33 nm lines. Combined with the low MW, it could cause the T_s to decrease drastically. Indeed, it was found to be 10 °C below the $T_{g\infty}$. Such an interpretation is not contradictory to the observed results.

The basis of the argument presented above for PS6k is that the bulk viscosity at T_s is low, i.e., below 10^9 Pa·s. Obviously, such an argument would not be valid for PS220k and PS1571k, whose viscosities are orders of magnitude higher. With surface tension as the only driving force there would be no measurable slumping in the experimental time window. On the other hand, such an argument is capable of explaining the PS15k and PS41k results, at least for the larger line widths of 300 and 600 nm, whose bulk zero

shear viscosity at T_s is on the order of 10^9 Pa·s. For example, the bulk viscosity of PS41k at 106.5 °C, calculated from the VFT model,[27] is about 2×10^9 Pa·s. The time constant of the surface wave decay is calculated (eq 1) to be about 2×10^4 s. In other words, 5% reduction in line height would require a mere 20 min. The point of this estimate is that T_s of the PS15k-300 nm and PS15k-600 nm as well as the PS41k pair are close to what would be expected from the bulk viscosity. To further examine this argument, the viscosity calculated from the H-Time measurement can be used.

In Figure 4, the relative height in logarithmic scale is plotted against time for films of PS41k from H-Time measurements. These films were heated to 4 °C above T_s and held constant. (The 33 nm film was taken further to 8° above T_s after ~700 min.) The result of 600 nm lines in this figure is a straight line except in the first 20 min (see inset of Figure 3). The linear regime suggests that the viscosity approaches a constant after beginning at a smaller or much smaller apparent value. The viscosity calculated for PS41k-600 nm in the linear regime is 1.2×10^9 Pa·s, about 1 order of magnitude higher than that predicted from the VFT model for the bulk (Figure 8). This viscosity increase is tentatively interpreted as a result of surface-induced chain alignment.[22]

In the 300 nm lines, the linear regime began when the height shrank to about 50% of the original. Once again, the viscosity in the linear regime derived from eq 2 is about 1 order of magnitude higher than the bulk zero shear viscosity for the same temperature and MW. The slumping started with apparent viscosity much lower than that in the linear regime. The negative slope reflecting the first few data points ($\tau \approx 100$ min) is about 5 times that in the linear regime ($\tau \approx 500$ min), which means the apparent viscosity at the onset of slumping is only one-fifth of that in the linear regime. In the case of the structure with a much smaller line width of 33 nm, an even larger reduction in the apparent initial viscosity is seen. Assuming that the few data points within the first 10 min is a part of single-exponential decay, the time constant would be about 20 min, which would correspond to a viscosity of about 2×10^9 Pa·s according to eq 1.[30] The viscosity at 98 °C, compared to the bulk zero shear viscosity of 7×10^{10} Pa·s, is more than 1 order of magnitude lower. It should be noted that this simple analysis cannot serve as evidence for the existence of a mobile surface layer. As discussed earlier, if there were a mobile surface layer to reduce the surface viscosity, T_s would be much lower in the PS6 600 and 300 nm films; therefore, this reduced apparent viscosity must have been caused by a stress that accelerates relaxation, perhaps due to spatial confinement. This possibility will be further discussed. After the first 20 min, the slumping speed decelerates and levels off between 500 and 700 min. At this point, as the temperature was raised by 4 deg to 102 °C, yet another faster decay, followed by a linear regime, was observed. The nonlinear regime immediately after raising the temperature suggests that the rapid relaxation at 98 °C is continued. The time constant for the linear regime is 1670 min, and the calculated viscosity is 7.3×10^{10} Pa·s, 1 order of magnitude higher than the corresponding zero shear bulk viscosity at 102 °C. In fact, the calculated viscosity of the linear regime for all the PS41k films is consistently an order of magnitude higher than that of the bulk (Figure 8). As will be shown later, there is also an increase in viscosity of between 1 and 2 orders of magnitude for the PS15k films (Figure 8). Also note that the surface viscosity of PS6k is estimated to be 2 orders of magnitude higher than that of the bulk. Taking all these results together, it can be surmised that as the molecular mass decreases, the surface viscosity would increase further beyond the bulk viscosity. Could this be due to surface-induced chain alignment?[22] If so, the shorter the chains, the more oriented the chains should be. Sum frequency generation measurement shows that the surface/interface causes the phenyl ring to orient either parallel or perpendicular to the surface normal.[31] Simulation supports the notion that the chains near a surface are somewhat flattened parallel to the surface.[32] Such orientation and conformation might enhance the inter- and intrachain interactions, especially in low MW PS. In a similar vein, McKenna[33] argued that "surface pinning" of entanglements could explain the observed larger rubbery modulus of ultrathin free-standing film than that of the bulk.

Alternatively, one may reason that the beginning of the slumping is in a transient state and the linear decay regime only appears in the later stage when the system stabilizes, yet it should be borne in mind that the surface tension induced stress and other possible driving forces have been acting on the lines right from the moment the imprinted films were released from the mold, not suddenly applied to the film. So the relevant question here is how rapidly the viscosity of the film can change. In fact, such nonlinear fast decay in the beginning of slumping has been observed by Soles et al.,[26] who attributed this behavior to residual stress. Since their samples were prepared by embossing and the imprinting condition probably did not allow sufficient time for the high MW molecules to relax, the residual stress explanation might be reasonable and suggests that a similar analysis of the current results is reasonable. However, it will be shown that even without residual stress, the nonlinear fast decay still exists for the PS1571k films.

The terminal relaxation time for PS41k at 150 °C calculated from eq 3 is a fraction of a second; therefore, the residual stress left in the films should be negligible. Consequently, the fast slumping in the beginning of H-Time measurement seen in Figure 4 cannot be due to residual stress. The possibility of non-Newtonian behavior must therefore be examined. Generally speaking, non-Newtonian behavior, such as shear thinning, is observed when the strain rate exceeds some critical value, viz., approximately the inverse of the terminal relaxation time of the polymer molecule.

For polystyrene, the empirical critical shear stress to crossover from linear regime to non-Newtonian or power law regime is

$$\sigma_c = \eta_0 \dot{\gamma}_0 \approx 0.6/J_e^\circ \tag{4}$$

where η_0, $\dot{\gamma}_0$, and J_e° are zero shear viscosity, critical shear rate, and steady-state recoverable creep compliance, respectively.[34] Take PS41k for example; at 107.5 °C, J_e° is $\sim 2 \times 10^{-6}$/Pa. This means that σ_c is about 0.3 MPa in steady state simple shear. While the stress state under consideration is not simple shear but rather surface wave decay, it is still reasonable to assume that there exists an analogous critical stress σ_c. When such a stress is exceeded, the apparent viscosity reduces, just like in the case of simple shear thinning, or it can simply be considered a kind of non-Newtonian behavior. For a sinusoidal surface wave, the surface tension induced stress is largest at the peaks and valleys of the wave and is determined by surface tension and the radius of curvature

$$P = \gamma \left(\frac{2\pi}{\lambda}\right)^2 \frac{h}{2} \tag{5}$$

where h is the peak-to-valley height. The maximum shear stress σ_m in the surface wave is half of P

$$\sigma_m = \gamma \frac{\pi^2}{\lambda} \frac{h}{\lambda} \tag{6}$$

If the initial maximum shear stress is larger than σ_c, non-Newtonian behavior would be observed: the apparent viscosity would be much lower than the zero shear viscosity, and the line height would decrease much faster than expected from the zero shear viscosity. In the meantime, the shear stress level in the surface wave (eq 6) would also reduce as the lines slump. At some

point of small line height h, the shear stress (eq 6) would fall below σ_c, at which point linear behavior would be restored and zero shear viscosity recovered. In the absence of other data, the steady-state simple shear result, i.e., eq 4, can be used as reference. The σ_c at 107.5 °C for PS41 is 0.3 MPa, while the maximum shear stress for 41k-300nm-rNIL-150C at the initial line height given by eq 6 is about 0.2 MPa if the waveform is assumed to be sinusoidal. The similarity between σ_m and σ_c suggests the likelihood of non-Newtonian behavior and thus provides a plausible explanation for the nonlinear fast slumping of this film in Figure 4. For the 33 nm lines, the radius of curvature at the top of the lines is smaller than half of the line width (Figure 1), which would easily produce shear stresses (eq 6) over 1 MPa. That is probably the reason why the linear regime was not reached until the line height was only several nanometers, and the shear stress given by eq 6 was less than σ_c. The important point here is that the stress from surface tension for structures ranging in size from submicrometers to a few tens of nanometers is in the order of 0.1−1 MPa and may prove large enough to move the system to cross over from the linear to the non-Newtonian regime, where the viscosity could be below the zero-shear viscosity.

The PS15k result is also very interesting. As shown in Figure 5, the H-Time curve of PS15k-300 nm is unlike what was observed in all other specimens; namely, there is a nonlinear *slower* slumping (or higher apparent viscosity) before the linear regime. (Two films were measured and produced similar results. Only one curve is shown in Figure 5.) From the linear regime, the slumping time constant is determined to be 210 min, corresponding to a viscosity of 2×10^9 Pa·s from eq 2. This viscosity is more than 1 order of magnitude higher than zero shear bulk viscosity at 103 °C. However, the larger apparent viscosity in the beginning of the slumping could be explained by a higher degree of order in chain alignment, which is very likely from the nanoimprinting process. As slumping proceeds, the chains lose some order but still maintain some surface-induced orientation to possess higher viscosity than the bulk.

On the other hand, PS15k-33 nm behaved very similarly to PS41k-33 nm, as can be seen in Figure 5. Notice that both measurements were performed at 98 °C. The higher MW PS41k presents the higher zero-shear viscosity, as indicated by the smaller absolute slope (thus slower slumping speed) in the linear regime. However, it is a little surprising to see that the PS41k lines slump faster in the beginning, before the two H-Time curves cross and enter the linear regime. As mentioned above, both samples were prepared in the same way, and the favorable nanoimprinting condition should have left no residual stress. Is it possible that PS41k-33 nm is in a deeper non-Newtonian regime? Since both films experience the same level of stress from surface tension, the higher MW film always has the larger viscosity than the lower MW one. Therefore, the faster slumping in PS41k-33 nm in the initial stage compared with PS15k-33 nm cannot be explained from the non-Newtonian behavior point of view. In addition, the T_s of PS41k-33 nm is about the same as that of PS15k-33 nm (Table 3), if not slightly lower, although the $T_{g\infty}$ of PS41k is 4 deg higher. With the analysis above, it is likely that the overall size of the molecules is the origin of the surprising observation.

Table 3 lists the radius of gyration (R_g) under theta condition for all the PS. Considering the fact that the diameter of PS41k molecules is close to 24 nm, the molecular coils must suffer a significant amount of deformation from its undisturbed state in order to fit into the 33 nm wide lines. This spatial confinement is expected to give rise to an entropic driving force for the lines to slump faster than can be expected from surface tension alone. This confinement effect can certainly explain the interesting comparison above between the PS41k and PS15k 33 nm lines. In addition to the simple idea of extreme confinement due to the disparity between the unperturbed polymer coil size and the line width, an earlier study showed that the relaxation time of a highly deformed polymer can be shortened by orders of magnitude.[35] The confined molecular coils in the line gratings are expected to be stretched along the surface, though whether the stretching direction is perpendicular or parallel to the lines is unknown. In either case, faster relaxation dynamics are expected in such deformed chains. Therefore, this activated relaxation would cause faster slumping in the PS41k-33 nm than the PS15k lines. As slumping proceeds, this effect should gradually disappear, and the relaxation should slow. Indeed, when the line-width narrows and the curvature increases, both the stress from surface tension and the confinement effect increase. The two factors work in concert to lower T_s and to cause faster slumping in the beginning of the slumping process.

The slumping behavior of the highest molecular mass material, PS1571k, is discussed next. Obviously, the viscosity of PS1571k remains high even well above the bulk $T_{g\infty}$. Using VFT parameters in the literature,[27] the bulk zero shear viscosity at 125 °C, 20 deg above the T_s for the 600 and 300 nm lines, is calculated to be 3×10^{11} Pa·s. At these dimensions, it is reasonable to think that the properties would approximate those of the bulk. Considering such a high bulk viscosity, there should not be any noticeable line height reduction in the measurement window if linear behavior was expected and surface tension the only driving force. However, the critical stress σ_c from eq 4 suggests non-Newtonian behavior, and thus the viscosity is much reduced from that of the bulk. The J_e° for PS1571 is about $10^{-4.86}$ Pa,[27] when the temperature is about 10 deg above $T_{g\infty}$ and beyond. That would suggest that σ_c is only about 40 kPa from eq 4, compared with surface tension generated shear stress at (eq 6) ~0.1 MPa for the 600 and 300 nm lines and ~1 MPa for the 33 nm lines. This comparison may reasonably explain some of the H-Time results in Figure 6, as non-Newtonian behavior causes the nonlinear fast slumping in the beginning, followed by the linear regime, which produces viscosity very close to the calculated bulk zero shear viscosity (Figure 8). Take film 1571k-300nm-Peel-115C, for instance: it was first taken to 113 °C, at which temperature the height decreased to 50% after only 10 min. Then the line height leveled off to about 30% of the initial height (~100 nm in absolute height) in another 200 min but remained essentially constant for the next 300 min. At this point, the system was very close to the linear regime. But, as the viscosity at 113 °C is very high, close to 10^{13} Pa·s,[27] the amount of flow should be negligible. When the temperature of the film was raised to 135 °C, the linear regime immediately appeared, with the slope of the exponential decay corresponding to the zero shear bulk viscosity.

However, the comparison of the stress level in the lines with σ_c can hardly explain the T_s for films of this high MW. J_e° of PS1571k for the bulk quickly decreases to about $10^{-8.5}$/Pa,[29] or the inverse of the glass modulus, when the temperature decreases from about 10 deg above $T_{g\infty}$ to $T_{g\infty}$. At $T_{g\infty}$, it is meaningless to use eq 4 to obtain σ_c, as such a calculation would produce a stress even larger than the yield stress of glassy PS at room temperature. In other words, the surface tension generated shear stress of less than 1 MPa is much smaller than the σ_c required for the onset of non-Newtonian behavior. Therefore, the surface tension generated shear stress cannot account for the low T_s observed on the PS1571k samples.

For such a high MW, it is always a concern whether the film preparation procedure was sufficient for removing the residual stress. The terminal relaxation time at 150 °C for PS1571k is about 6 h, according to eq 3. This relaxation time is much longer than the nanoimprinting time, which was about 10 min. Soles et al.[26] also noted the possibility of residual stress from unfavorable fabrication conditions and then attributed similar fast nonlinear slumping for high molecular mass as seen in Figure 6 to

residual stress. The existence of residual stress in 1571k-300nm-rNIL-150C, 1571k-300nm-Peel-115C, and 1571k-300nm-Peel-155C, whose H-Time measurement is shown in Figure 6, is possible. However, it will be shown here that the residual stress is not the main reason to cause the low T_s, and it is only part of the contribution to the nonlinear fast slumping in the beginning.

The residual stress can be effectively removed when more aggressive annealing condition is utilized. Film 1571k-300nm-Peel-180C and 1571k-300nm-Peel-190C were annealed at 180 °C for 24 h and 190 °C for 48 h, respectively. These two films produced almost identical results in both H-Temp and H-Time measurements (Figures 3 and 6). At 180 °C, the terminal relaxation time of PS1571k is 9 min, while at 190 °C, it is 4 min. Therefore, residual stress should have been completely removed for these two films. Yet, there is only a very modest 2° increase in T_s, compared with 1571k-300nm-rNIL-150C. And the films still experienced fast nonlinear slumping upon being raised to 135 °C after the H-Temp measurement that ended at 130 °C (Figure 6). These two results strongly suggest that the fast nonlinear slumping is not an aftermath of the residual stress. On the other hand, the removal of residual stress did prompt an earlier onset of the linear slumping regime. In Figure 6, the onset of linear slumping regime for 1571k-Peel-155C was around 40% of relative height (absolute height at about 100 nm). When the film was annealed at the lower temperature of 115 °C for 1571k-300nm-Peel-115C, presumably with a higher level of residual stress, the onset of the linear regime was brought down to 30% in relative height. When all residual stress was removed in 1571k-300nm-Peel-180C and 1571k-300nmPeel-190C, the onset of the linear regime was moved up to 50% in relative height.

The onset of the linear slumping regime is also reflected in H-Temp measurements. As discussed earlier, measurable slumping in the *linear* regime for this high molecular mass PS was only achieved when the temperature was high, e.g., above 130 °C, where the stress associated with surface tension overcame the zero shear viscosity of the film. The slumping by this mechanism is so slow as to be undetectable near T_s, i.e., around 100 °C. However, some combination of driving forces, including residual stress, enabled the lines to slump, and a major line height decay took place in a narrow temperature window of 5°−10°. The result was then a wide temperature window wherein a plateau occurred between the fast slumping near T_s and slow slumping in the linear regime at much higher temperature. In Figure 3, it can be seen that the plateau level for the 33 nm lines is lower than that of the 300 nm lines. This is reasonable. Even for the 1571k-33nm-rNIL-195C, which had been annealed in the nanoimprinter for 10 min and should be without residual stress, the plateau level is only around 10% in relatively height, or 6 nm. Figure 7 shows H-Time measurement at 135 °C for 1571k-33nm-Peel-180C, which had been annealed at 180 °C for 24 h. The onset of the linear slumping regime is very close to the plateau level in the H-Temp measurement of 1571k-33nm-rNIL-195C, as both films had been subjected to an aggressive annealing process to remove the residual stress. The viscosity revealed from this linear regime also agrees with the bulk zero shear viscosity.

From the above discussion on PS1571k, it was shown that residual stress and surface tension associated stress could not explain all the slumping behavior. Analysis of the stress from surface tension does show the possibility of non-Newtonian behavior at about 10 deg above T_s and beyond. But this low stress compared with σ_c can hardly explain the low T_s value, as no non-Newtonian behavior is expected very close to and below the bulk $T_{g\infty}$. Residual stress may have been responsible for part of the fast slumping near T_s, but even without residual stress, the lines still slumped quite readily with slightly larger T_s.

The other existent slumping driving force that must be further considered is the spatial confinement effect. For PS1571k, the molecular coils should be highly distorted even for lines as wide as 600 nm. Viscous flow might not be the mechanism behind the slumping occurring at such a low temperature. As temperature approaches the bulk T_g, the distorted chains confined in the lines may gain enough mobility to rearrange due to the enhanced relaxation,[35] thus causing the line to slump.

It is possible to make a film with little confinement effect even for PS1571k, if the line width is sufficiently large. To this end, 1571k-8μm-Peel-180C was fabricated. PS solution was spin-cast onto the mold with 8 μm wide trenches. Multiple casting was needed to fill the trenches 1 μm in height. The film was then annealed in vacuum at 180 °C for 24 h. Figure 3 shows the H-Temp measurement of this film. Other than a 2% kink around 112 °C, the line height remained stable all the way to 147 °C. At 147 °C, H-Time measurement for a short duration of 2 h followed the H-Temp measurement. The line height was found to relax in the linear regime, and the viscosity derived, 2×10^9 Pa·s, also agrees well with that of the bulk (Figure 8).

With the result of PS41k and PS1571k interpreted, the PS220k data can now be understood. H-Time measurement of PS220k-300 nm produced viscosity in good agreement with the bulk, as shown in Figure 8. The low T_s value, just like PS1571k, is apparently due to the spatial confinement of the large molecular coils.

It is worth noting that non-Newtonian behavior, such as shear thinning, has been used to interpret some behaviors in polymer thin films. Dutcher et al.[24] found that shear thinning made it possible for holes to grow in free-standing PS films even below T_g for films of high molecular mass. Using the analysis presented in this paper, one can immediately find that the stress at the edge of growing holes in Dutcher's work is much lower than the critical stress calculated from eq 4. (As the free-standing film is bulklike from the viscosity point of view, bulk compliance is used in the calculation as well.) In other words, it is difficult to invoke stress as the cause for the apparent shear thinning. In addition, the hole growth was observed by Dutcher in the vicinity of T_g and, in many instances, below the bulk T_g. Shear thinning in this temperature window is implausible in the case of bulk polymers. One possible alternative interpretation may involve the spatial confinement argument presented in this paper. The thicknesses of free-standing films studies by Dutcher et al. are comparable to R_g of the molecules. Consequently, the molecules may exhibit enhanced relaxation behavior, which can also facilitate the growth of holes and flow the material from the holes evenly to the rest of films.

There are also reports of reduced viscosity compared to bulk as film thickness decreases.[20,21] In both experiments, the observed reduction in apparent viscosity was interpreted as the existence of a mobile surface layer. However, in both cases, the stress level in the thin film exceeds the critical stress calculated from eq 4. Since the temperatures in these two cases were well above T_g, non-Newtonian behavior, such as shear thinning, can be an alternative interpretation for the reduced apparent viscosity. In addition, the films thickness where apparent viscosity decreased in these two studies compared to the molecular size also invites the spatial confinement argument.

A further point that can be made is that the mechanism behind non-Newtonian behavior is commonly thought to be due to the loss of entanglement as the shear rate exceeds the inverse of the relaxation time. Loss of entanglement could occur from unfavorable chain arrangement.[36] For example, one may argue that the entanglement density is lower for the molecules at polymer surface as there are no molecules from the free surface side to penetrate and entangle the molecules at the surface. This type of loss of entanglement can also cause decreased viscosity. If such mechanism exists at all, it is not evident in the results presented here. As can be seen, in the later stage of slumping where the

viscosity recovers to the zero shear (no entanglement loss) value, the viscosity agrees with that of the bulk or, in the case of low MWs, is 1 order of magnitude higher. Therefore, the loss of entanglement, if any, has nothing to do with the surface. In fact, the opposite—enhanced entanglement along the surface—appears to have happened, as the viscosity results of PS15k and PS41k would suggest. The molecules on the surface may suffer a loss in entanglement from the absence of molecule above the free surface, but the improved packing of molecules parallel to the surface, on the other hand, seems to have more than made up for that loss.

Conclusion

Line gratings with line width as small as 33 nm were fabricated on PS surface of various molecular masses ranging from below the entanglement molecular mass to well above. When temperature was raised through the bulk glass transition temperature, the lines on the polymer surface began to slump at a temperature T_s. For any given molecular mass, T_s decreased with the reduction in line width. This trend signals that as the feature size of nanostructure on polymer surface decreases, the thermomechanical stability will be compromised. The seemingly simple T_s trend with grating line width cannot be interpreted as the effect of a mobile surface layer. In fact, the present work strongly suggests that the viscosity of the surface is either consistent with that of the bulk polymer for high molecular mass PS or 1−2 orders of magnitude higher than that of the bulk. With this finding and the relatively high T_s compared with the bulk $T_{g\infty}$ for the low molecular mass PS gratings, it can be concluded that the mobile surface layer does not play a significant role in the decrease of T_s with the reduction in structure line width. The surprising high viscosity found in the low molecular mass PS surface is suggestive of enhanced entanglement, perhaps from surface induced molecular orientation, which would increase the amount of interactions per molecule.

In observing the kinetics of the line grating slumping, it was found that the surface tension induced stress plays a role in the decrease of T_s. As the line width narrows, the stress caused by surface tension increases. Qualitatively speaking, when the stress exceeded some critical value, non-Newtonian behavior resulted in the form of lowered apparent viscosity. The semiquantitative analysis shows that the stress induced by surface tension is capable of causing such non-Newtonian behavior, which may have produced the nonlinear fast slumping when the stress in the line gratings was large. Only when the line height reduced to certain level and the surface tension induced stress became lower than the critical stress did the linear behavior recover. Since non-Newtonian behavior is only expected for polymer flow at temperatures well above $T_{g\infty}$ due to the generally low surface tension generated stress, it might have little relevance to the low T_s very close to $T_{g\infty}$, especially for the high molecular mass PS line gratings. With careful study of the line grating slumping kinetics, it was also found that the size of the molecule played a very strong role. With molecular coils of a given size confined in a narrow space comparable to or even smaller than the coil size, the entropic force is expected to rise, giving additional driving force for the structure to slump. Spatial-confinement-induced molecular deformation could also enhance the relaxation rate, even quite significantly, which would then allow the nanostructure on the polymer surface to deform in the vicinity of $T_{g\infty}$.

Acknowledgment. This research is funded by NSF (CMMI-0728352). Special acknowledgment goes to Zeiss Excellence Center at Calit2, UC Irvine, for providing SEM support. We also appreciate the productive discussion with Dr. Christopher Soles and Dr. Wen-Li Wu in Polymer Group, National Institute of Standards and Technology, Gaithersburg, MD.

References and Notes

(1) Reiter, G. *Phys. Rev. Lett.* **1992**, *68*, 75–78.
(2) Keddie, J. L.; Jones, R. A. L.; Cory, R. A. *Europhys. Lett.* **1994**, *27*, 59–64.
(3) Ellison, C. J.; Torkelson, J. M. *Nat. Mater.* **2003**, *2*, 695–700.
(4) Forrest, J. A.; Dalnoki-Veress, K.; Dutcher, J. R. *Phys. Rev. E* **1997**, *56*, 5705–5716.
(5) Ngai, K. L. *Eur. Phys. J. E* **2002**, *8*, 225–235.
(6) Doruker, P.; Mattice, W. L. *Macromolecules* **1999**, *32* (1), 194–198.
(7) de Gennes, P. G. *Eur. Phys. J. E* **2000**, *2*, 201–203.
(8) Stevenson, J. D.; Wolynes, P. G. *J. Chem. Phys.* **2008**, *129*, 234514.
(9) Priestley, R. D.; Ellison, C. J.; Broadbelt, L. J.; Torkelson, J. M. *Science* **2005**, *309*, 456–459.
(10) Wallace, W. E.; Fischer, D. A.; Efimenko, K.; Wu, W. L.; Genzer, J. *Macromolecules* **2001**, *34*, 5081–5082.
(11) Rotella, C.; Napolitano, S.; Wübbenhorst, M. *Macromolecules* **2009**, *42*, 1415–1417.
(12) Toney, M. F.; Russell, T. P.; Logan, J. A.; Kikuchi, H.; Sands, J. M.; Kumar, S. K. *Nature* **1995**, *374*, 709–711. Tocha, E.; Schonherr, H.; Vancso, J. *Soft Matter* **2009**, *5*, 1489–1495.
(13) Roth, C. B.; Dutcher, J. R. *J. Electroanal. Chem.* **2005**, *584*, 13–22.
(14) Forrest, J. A. *Eur. Phys. J. E* **2002**, *8*, 261–266.
(15) Fakhraai, Z.; Forrest, J. A. *Science* **2008**, *319*, 600–604.
(16) Buck, E.; Petersen, K.; Hund, M.; Krausch, G.; Johannsmann, D. *Macromolecules* **2004**, *37*, 8647–8652.
(17) Kerle, T.; Lin, Z.; Kim, H. C.; Russell, T. P. *Macromolecules* **2001**, *34*, 3484–3492.
(18) Mundra, M. K.; Donthu, S. K.; Dravid, V. P.; Torkelson, J. M. *Nano Lett.* **2007**, *7*, 713–718.
(19) Chou, S. Y.; Krauss, P. R.; Renstrom, P. J. *Appl. Phys. Lett.* **1995**, *67*, 3114–3116. Chou, S. Y.; Krauss, P. R. *Microelectron. Eng.* **1997**, *35*, 237–240.
(20) Bodiguel, H.; Fretigny, C. *Macromolecules* **2007**, *40*, 7291–7298. Bodiguel, H.; Fretigny, C. *Phys. Rev. Lett.* **2006**, *97*, 266105.
(21) Masson, J. L.; Green, P. F. *Phys. Rev. E* **2002**, *65*, 031806.
(22) Hamdorf, M.; Johannsmann, D. *J. Chem. Phys.* **2000**, *112*, 4262–4270.
(23) Kim, H.; Ruhm, A.; Lurio, L. B.; Basu, J. K.; Lal, J.; Lumma, D.; Mochrie, S. G. J.; Sinha, S. K. *Phys. Rev. Lett.* **2003**, *90*, 068302.
(24) Roth, C. B.; Dutcher, J. R. *Phys. Rev. E* **2005**, *72*, 021803. Roth, C. B.; Nickel, B. G.; Dutcher, J. R.; Dalnoki-Veress, K. *Rev. Sci. Instrum.* **2003**, *74*, 2796–2804.
(25) Huang, X. D.; Bao, L. R.; Cheng, X.; Guo, J.; Pang, S. W.; Yee, A. F. *J. Vac. Sci. Technol. B* **2002**, *20*, 2872–2876.
(26) Ro, H. W.; Ding, Y. F.; Lee, H. J.; Hines, D. R.; Jones, R. L.; Lin, E. K.; Karim, A.; Wu, W. L.; Soles, C. L. *J. Vac. Sci. Technol. B* **2006**, *24*, 2973–2978. Jones, R. L.; Hu, T.; Soles, C. L.; Lin, E. K.; Reano, R. M.; Pang, S. W.; Casa, D. M. *Nano Lett.* **2006**, *6*, 1723–1728.
(27) Majeste, J. C.; Montfort, J. P.; Allal, A.; Marin, G. *Rheol. Acta* **1998**, *37*, 486–499.
(28) Chee, K. K. *J. Appl. Polym. Sci.* **1998**, *70*, 697–703.
(29) Plazek, D. J.; O'Rourke, V. M. *J. Polym. Sci., Part A-2* **1971**, *9*, 209–243.
(30) Note that the initial line width is 33 nm and the wavelength is 200 nm. Throughout the surface wave decay, the space in between lines is wider than the lines (see Figure 1d). To estimate viscosity using eq 2, 150 nm is assumed for the wavelength near the end of the slumping, and 75 nm is assumed in the beginning.
(31) Gautam, K. S.; Schwab, A. D.; Dhinojwala, A.; Zhang, D.; Dougal, S. M.; Yeganeh, M. S. *Phys. Rev. Lett.* **2000**, *85*, 3854–3857.
(32) Doruker, P.; Mattice, M. L. *Macromolecules* **1998**, *31*, 1418–1426.
(33) O'Connell, P. A.; McKenna, G. B. *Eur. Phys. J. E* **2006**, *20*, 143–150. O'Connell, P. A.; McKenna, G. B. *Science* **2005**, *307*, 1760–1763.
(34) Graessley, W. W. *Adv. Polym. Sci.* **1974**, *16*, 1–179.
(35) Yee, A. F.; Bankert, R. J.; Ngai, K. L.; Rendell, R. W. *J. Polym. Sci., Part B: Polym. Phys.* **1988**, *26*, 2463–2483. Ngai, K. L.; Roland, C. M.; Yee, A. F. *Rubber Chem. Technol.* **1993**, *66*, 817–826.
(36) Si, L.; Massa, M. V.; Dalnoki-Veress, K.; Brown, H. R.; Jones, R. A. L. *Phys. Rev. Lett.* **2005**, *94*, 127801.